Preparation, Characterization and Catalytic Testing of GePt Catalysts

N. Győrffy[a], I. Bakos[b], S. Szabó[b], L .Tóth[c], U. Wild[d], R. Schlögl[d], Z. Paál[a*]

[a]Institute of Isotopes, CRC, Hungarian Academy of Sciences, P. O. Box 77, Budapest, H-1525 Hungary;
[b]Institute of Material and Environmental Chemistry, CRC, HAS, POB. 17, Budapest, H-1525, Hungary
[c]Institute of Technical Physics and Materials Science, Hungarian Academy of Sciences, P. O. Box 49, Budapest, H-1525 Hungary;
[d]Fritz-Haber-Institut der MPG, Faradayweg 4-6, D-14195 Berlin, Germany.

[*] Corresponding author: e-mail paal@iki.kfki.hu,

Abstract

Unsupported and SiO$_2$ supported GePt bimetallic catalysts were prepared by depositing Ge on to Pt underpotentially. Surface-sensitive cyclic voltammetry of Pt black indicated that Ge covered ca. 40-45 % of the Pt surface, whereas XPS showed just ~96 % Pt and ~4 % Ge (normalized to Pt+Ge=100 %). High-resolution Ge map of GePt black obtained by Energy Filtered TEM (EFTEM) showed Ge scattered in the near-surface regions. Both catalysts were tested in hexane (nH) transformation reactions between 543 and 603 K and 60 to 480 Torr H$_2$ pressure (with 10 Torr nH), and compared with the parent Pt catalysts. GePt/SiO$_2$ catalyst was also tested with methylcyclopentane (MCP). Adding Ge to Pt/SiO$_2$ lowered the activity; the opposite effect was observed with GePt black. The selectivities of saturated products on bimetallic catalysts decreased, while those of hydrogenolysis products, benzene and hexenes increased in nH transformations over supported catalyst. The reverse effects were observed over the black samples where addition of Ge prevented accumulation of adventitious carbon. Ring opening was the main reaction with MCP, together with some fragments, benzene and unsaturated hydrocarbons. Ring opening of MCP became more selective with decreasing temperature and increasing hydrogen pressure. Ge on GePt black blocked contiguous Pt sites favoring the formation of coke precursors. The different catalytic behavior of GePt/SiO$_2$ indicated somewhat different Pt–Ge interaction(s).

1. Introduction

Platinum is the typical active metal component in bifunctional catalysts of naphtha reforming for producing high-octane gasoline [1,2,3]. It is responsible for hydrogenation– dehydrogenation reactions [4] but also for producing C$_5$ and C$_6$ cyclic products in hydrogen excess as well as the opening of the C$_5$ rings [5]. Useful reactions are accompanied by the formation of polymeric carbonaceous deposits ("coke") on contiguous Pt surfaces. Introducing second metals (such as Re, Sn, Ge) would divide the metal surface into smaller islands, preventing thus polymerization of unsaturated intermediates to form a two-dimensional layer of potential coke precursors. At the same time small metallic ensembles required for the production of cyclic compounds as well as isoalkanes [6] were still present. The added second components have, as a rule, low catalytic activity (to this end, Re is sulfided). The character of the interaction of these second metals with platinum has not been clarified, yet. There is no agreement in the literature

whether a purely geometric effect (as outlined above) or electronic interactions take place and which of them is the main reason of the beneficial effect of the second metal [6,7,]. The advocates of both views presented experimental results for supporting their theories; for example, Goldwasser et al. [8] attributed the improved catalytic properties of precalcined Pt-Ge/Al$_2$O$_3$ catalysts merely to geometric effects, whereas Borgna et al. [9] detected an electronic interaction between Pt and Ge by EXAFS. The oxidation state of Ge [7] and the possible existence of Pt-Ge intermetallic compounds [10] during catalytic reaction have been studied, but these problems still represent a matter of question. Thus, the interaction of the two metals (and the resulting catalytic effect) is a problem influenced by several factors.

In addition to "classical" methods of preparing bimetallic catalysts [6], the methods of "controlled surface reaction" (CSR) is becoming more and more widespread. These include reaction of an organometallic compound with hydrogen chemisorbed on the surface of the first metal [11] as well as underpotential deposition of a second metal on to the surface of the catalytically active component of the monometallic catalyst [12], i.e., Pt in our case.

Our recent paper [13] used organometallic grafting for preparing Pt-Ge/Al$_2$O$_3$ catalysts with various Ge content. The amount of Ge added was expressed there in terms of monolayers: e.g., "**Ge1/12"** means adding 1/12 Ge to Pt while "**Ge 1"** means 1 monolayer Ge on Pt. A "surface bimetallic system" arose with Ge less than one monolayer whereas a "bulk bimetallic system" started to form with 1 and 2 monolayers of Ge. Catalytic tests with hexane, cyclohexene and benzene indicated a selective deposition of Ge on high-coordination sites, blocking (100) and (111) sites. The latter configuration represents the active centers for aromatization [14]. Samples with low Ge content (Ge 1/8 and Ge 1/2) were most active in hexane transformation. Pt-Ge catalysts produced also saturated hydrocarbons with highest selectivities: mostly methylcyclopentane (MCP) at lower p(H$_2$) and isoalkanes at higher p(H$_2$) values. This agreed with the report by Mariscal et al. [7]: maximum activity and best isomer selectivities in heptane reactions appeared at intermediate Ge concentrations.

The present study deals with two Ge-Pt catalysts prepared with underpotential deposition of Ge [12], like in the case of Pt-Rh catalysts [15,16]. These catalysts were characterized by cyclic voltammetry, electron spectroscopy and electron microscopy, as well as test reactions of hexane and methylcyclopentane. All of their "skeletal" reactions can be catalyzed also by the metallic function only [4,17], (even if some reactions are more rapid in the presence of the acidic function). The catalytic reaction itself will also be used to obtain reliable information on the actual state of the surface of the metal catalyst [18]. Supported and unsupported Ge-Pt samples were compared with their monometallic parent catalysts.

2. Experimental

2.1. Catalyst preparation

The parent unsupported catalyst was Pt black prepared by reduction of H$_2$PtCl$_6$ with aqueous hydrazine [19] and sintered in H$_2$ at 473 K [20]. A nonacidic material: SiO$_2$ has been selected for the support of Pt, since the second metal (as Ge oxide) could also interact with the acidic function of the bifunctional reforming catalysts [21]. A well-characterized 3.1 % Pt/SiO$_2$ (InCat-1 [22]) was used as the parent catalyst. It was prepared by ion exchange using [Pt(NH$_3$)$_4$]Cl$_2$ at pH = 10 [23] and used for comparison as a monometallic Pt/SiO$_2$ catalyst. The specific surface of the silica support was 300 m^{2}g^{-1} [22,23,24].

The second metal, Ge was deposited on both parent platinum catalysts via the ionization of pre-adsorbed hydrogen (a method based on the underpotential deposition of metals on foreign metal surfaces) [12,15,16]. 0.1 g of Pt catalyst, covered with adsorbed hydrogen was modified with Ge by exchanging the 1 mol L^{-1} HCl supporting electrolyte in the reactor with the same volume of deoxygenated 1 M HCl stock solution saturated with GeO$_2$. The hydrogen adsorbed on Pt parent catalyst reacted with the dissolved Ge, and the electrode potential of the catalyst gradually rose up to about 0.4 V (with respect to a hydrogen electrode in also 1 M HCl), showing that all of the adsorbed hydrogen reacted with Ge. When the reaction of hydrogen (adsorbed on the catalyst) with germanium ions was completed, the catalyst was washed free of germanium ions with deoxygenated 0.2 mol dm^{-3} HCl, then with triply distilled water. Finally, the wet catalyst modified with adsorbed Ge was dried in deoxygenated N$_2$ gas flowing through the reactor while the reactor was warmed with infrared lamp.

2.2. Catalyst characterization

2.2.1. Electrochemical characterization

As reported for Pt-Rh catalyst, cyclic voltammograms (CV) of 5 mg Pt and Pt-Ge catalyst were measured at room temperature in a three-compartment electrochemical cell using 0.5 mol dm^{-3} H$_2$SO$_4$ electrolyte. A more detailed description of this procedure can be found in our earlier paper [25]. The upper section of the voltammogram (anodic branch, above the abscissa) corresponds to oxidative processes, whereas the reverse (reductive) processes appear on the cathodic branch, below the abscissa. The electric insulator character of the SiO$_2$ prevented the CV study of the supported catalyst.

2.2.2. XPS

Surface composition was determined by X-ray Photoelectron Spectroscopy (XPS). A Leybold LHS 12 MCD instrument was used with a Mg K_α anode for XPS (pass energy, PE = 48 eV) [19,26,27,28]. The binding energy (BE) was calibrated to the Au $4f_{7/2}$ line (BE = 84.0 eV). Pt 4f, O 1s, C 1s and Ge $3p_{3/2}$ lines were monitored. Atomic compositions were determined using the SciPlot spectrum evaluation program (©M. Wesemann, Berlin) and literature sensitivity factors [29]. The samples were treated in the preparation chamber with H_2 and transferred to the spectrometer chamber without contacting it with air.

2.2.3. Transmission electron microscopy

Transmission electron microscopy was used to estimate the particle shape and provide information on their composition. The catalyst sample was ground in an agate mortar, then dispersed in ethanol and dropped onto holey carbon grid. For conventional TEM studies a Philips CM20 electron microscope was used, at 200 kV accelerating voltage. This microscope was capable of carrying out Energy Dispersive X-ray Spectrometric (EDS) analysis on thin specimens with the attached X-ray detector. A 300 kV electron microscope of the type JEOL 3010 with a resolving power of 0.17 nm and supplemented with a GATAN Tridiem energy post-column energy filter was also applied for high-resolution imaging. This equipment is suitable for acquiring images using electrons of specific energy loss (Energy Filtered TEM, EFTEM) creating thus so-called elemental maps (with a resolution of a few nm). For elemental mapping of germanium the Ge-L2,3 edge was used with the 3 energy windows (each of 60 eV slit width), centered at 1247 eV (post-edge), 1117 eV (pre-edge1) and 1177 eV (pre-edge2), respectively.

2.2.4. Catalytic test reactions

The catalytic experiments were carried out in a closed-loop glass reactor. A CP 9001 gas chromatograph with a 50 m CP-Sil 5CB capillary column and FID detector was attached to the system [30]. Batches of 9.2 and 9.7 mg of silica supported and 16.5, 20 mg of unsupported GePt and Pt catalysts, respectively, were placed in the reactor. **GePt/SiO₂** catalyst was tested in hexane (nH) transformation and methylcyclopentane (MCP) ring-opening reactions, while **GePt** black was tested only with hexane. Standard nH and MCP pressures of 10 Torr (1 Torr = 0.133 kPa) were used while the hydrogen pressures varied between 60 and 480 Torr. The reaction temperatures ranged from 513 to 603 K in MCP reactions. The temperature range in hexane transformation was 543 to 603 K. Samples were taken after 5 min. Each run was followed by regeneration with O_2 (50 Torr, 2 min) and H_2 (150 Torr, 3 min) at the temperature of the preceding run. The catalytic activity
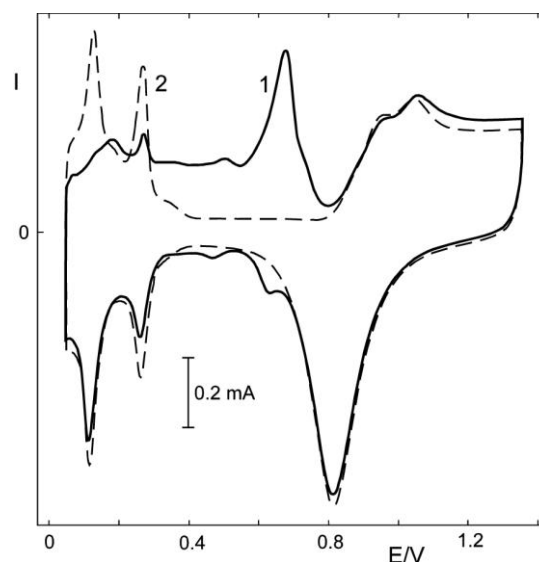
Fig. 1: Cyclic voltammogram of the **GePt** catalyst (1), and the bare **Pt** (2) after dissolution of germanium. Sweep rate: 2 mV s⁻¹

was expressed as turnover frequency (TOF, h⁻¹) using dispersion data published earlier for Pt black [31]. The dispersion values of supported **Pt** and **GePt** catalysts were measured by H_2 adsorption at room temperature (298 K): 52 % for Pt/SiO₂ and 47 % for GePt/ SiO₂.

3. Results

3.1. Catalyst characterization

3.1.1. Electrochemical characterization

Figure 1 (curve 1) shows the cyclic voltammogram of the black **GePt** catalyst. Curve 2 represents the bare platinum surface, which was obtained after dissolution of germanium by 5 potential cycles between 50 and 1350 mV. Similar voltammograms were measured during electrochemical investigation of germanium ad-atoms on polycrystalline [32] and on some single crystal platinum electrodes [33,34]. Peaks between 50 and 300 mV correspond to the ionization (anodic side, above the abscissa) or deposition (cathodic side, below the abscissa) of adsorbed hydrogen. Peaks (or waves and humps) above 300 mV potential in the anodic side of the voltammogram (1) can be assigned to the oxidation and to the oxidative desorption of germanium.

Fig. 1 shows that hydrogen adsorption is suppressed by the germanium adatoms. The surface coverage of the Pt catalyst by Ge can be estimated from the decrease of hydrogen adsorption capacity. Comparing the two voltammograms, about 40-45 % of the Pt surface seems to be blocked by the germanium. If we suppose that site requirement of an adsorbed Ge atom corresponds to two hydrogen adsorption sites – as was reported in the case of polycrystalline Pt

[32] and Pd [35] – the Ge:Pt atomic ratio on the surface can be about 1:5.

3.1.2. XPS

Photoelectron spectra of the unsupported **GePt** catalyst were measured in three states: "as is", after H_2 treatments: at 300 K and at 473 K. The atomic compositions are summarized in Table 1. The Ge coverage of ca. 40 % observed by cyclic voltammetry seems to be valid in the catalyst contacting with an aqueous electrolyte solution. This value is valid for the whole information depth (of a few atoms). That is the reason why CV – that method scanning just the outmost surface layer – detected more Ge. The filtered and dried Pt-Ge shows ca. 96 % Pt and 4 % Ge (when normalized to Pt+Ge=100 %). The "as received" catalyst contained conspicuously low amounts of "adventitious carbon"; thus the electrochemical procedure must have removed rather much carbon. The residual C was mostly in graphitic state, as reported for the cleanest Pt black [19]. Hydrogen treatment increased the amount of C in the information depth, in agreement with earlier studies: H penetrating into subsurface positions of Pt causes structural rearrangement and "pushes" carbon on to the surface [28,36]. Decomposing the C 1s peak showed the same components as reported also for Pt black [28]; most carbon was present as graphene or graphite (~284.2 – ~284.6 eV) with small amounts of individual C atoms (BE ~283.8 eV) and aliphatic polymer (C_xH_y, BE ~285.6 eV). Oxidized C (BE > 286 eV; typically a minor component [36]) was absent. The shape of C 1s lines was similar after each treatment, i.e., the ratio of the above-mentioned components did not change noticeably.

Figure 2a shows the Ge $3p_{3/2}$ lines. Mostly Ge salt (presumably chloride) was detected in the untreated catalyst. H_2 reduced most Ge even at 300 K. GeO_2 also appeared, presumably as a result of reaction of Ge and oxygen chemisorbed over Pt during storage in air [19]. The Pt 4f peaks in the "as is" state and after H_2 treatments appeared at the same binding energy, corresponding to Pt^0 (Figure 2b), indicating a clean metallic state with no Pt–O interaction, not even with "chemisorbed oxygen" ($\Delta E \sim 0.8$ eV [19]), unlike to what was reported for PtRh [15]).

The insulator character of supported catalyst caused considerable binding energy shift and peak broadening in the XPS peaks of the active components present in small concentrations, as observed with EUROPT-1 (6 % Pt) [37]. Still lower and uncertain signals could be expected with our 3 % Pt, (Ge may even be around the detection limit – see below, Section 3.1.3.), no XPS measurement was attempted with this sample.

3.1.3.Transmission electron microscopy

The left-hand panel of Figure 3 shows transmission electron microscopic (TEM) image of a selected area of

Table 1: Comparison of the surface composition of GePt catalyst measured by XPS in the "as is" state and after hydrogen treatments at 300 and 473 K.

| Treatments	GePt surface composition (%)			
	Pt 4f	**Ge 2p3/2**	**C 1s**	**O 1s**
GePt "as is"	81.8	3.3	4.4	10.5
H_2 (300 K)	72.5	2.3	16.8	8.4
H_2 (473 K)	76.9	2.4	15.0	5.7

untreated **GePt** black taken with elastically scattered electrons (zero loss image). On this micrograph, an aggregate of individual crystallites with diameters up to ~50 nm [20] can be observed. The panels on the right-hand side present Pt-map (Fig 3a) and Ge map (Fig 3b), respectively, obtained by EFTEM of the same area. Not surprisingly, the Pt map shows everywhere the predominance of the main component: Pt. The Ge elemental map represents a quantity of Ge hardly exceeding (or below) the detection limit. However, the image might best be interpreted as a very thin Ge layer partly covering the free surface of the Pt grains. This is supported by the enhanced Ge signal at some edges of the Pt particles in tangential view through the geometrical effect of a thin surface coating [26]. Similar thin Ge islands may exist on other faces of Pt grains but they remain invisible due to the low signal to noise ratio. The conclusion is the Ge covers the surface of Pt grains more or less unevenly.

The TEM picture of **GePt/SiO$_2$** was very similar to that of PtRh/SiO$_2$ (using the same InCat-1 as parent catalyst) published earlier [16]. EM of the present sample showed no morphological difference in the metallic particles. The small amount of Ge on this supported catalyst was below the sensitivity limit of the EFTEM.

3.1.4. Catalytic tests

3.1.4.1. *GePt/SiO$_2$ in the catalytic reaction of hexane*

Figure 4 illustrates how the turnover frequencies for hexane conversion changed on both catalysts as a function of temperature and hydrogen pressure. The turnover frequencies on the bimetallic GePt samples were much lower. The presence of Ge decreases the continuous Pt surface and decreases the number of active sites. This correlates well with the dispersion determined by hydrogen chemisorption, its value decreasing from 52 % to 47 %. This means that adding a second metal to Pt may also exert a hampering effect in the *overall* activity. Thus, the total number of sites active in hydrogen chemisorption decreases, but, at the same time, sites possessing particular catalytic properties are created. This will alter the product distribution (Table 2). Isomers, hydrogenolysis products ($<C_6$) and MCP were formed from hexane on each catalyst and also benzene and unsaturated hydrocarbons (mainly 1-hexene and *cis*-2-hexene) were observed. Isomerization and C_5-cyclization were the main reactions on both catalysts. Selectivity of
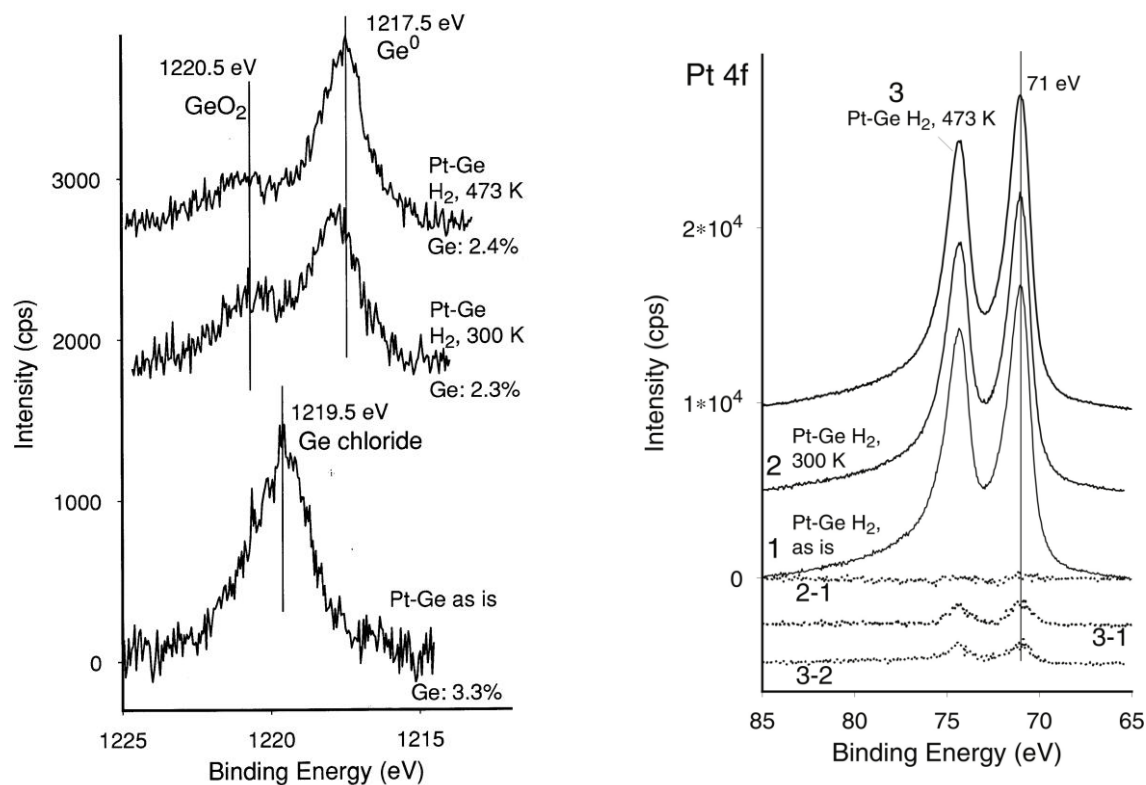
Fig. 2a: Ge 2p 3/2 XP spectra for **GePt** black catalyst after different treatments. **Fig. 2b**: Pt 4f XP spectra for **GePt** black catalyst after different treatments and corresponding difference spectra.
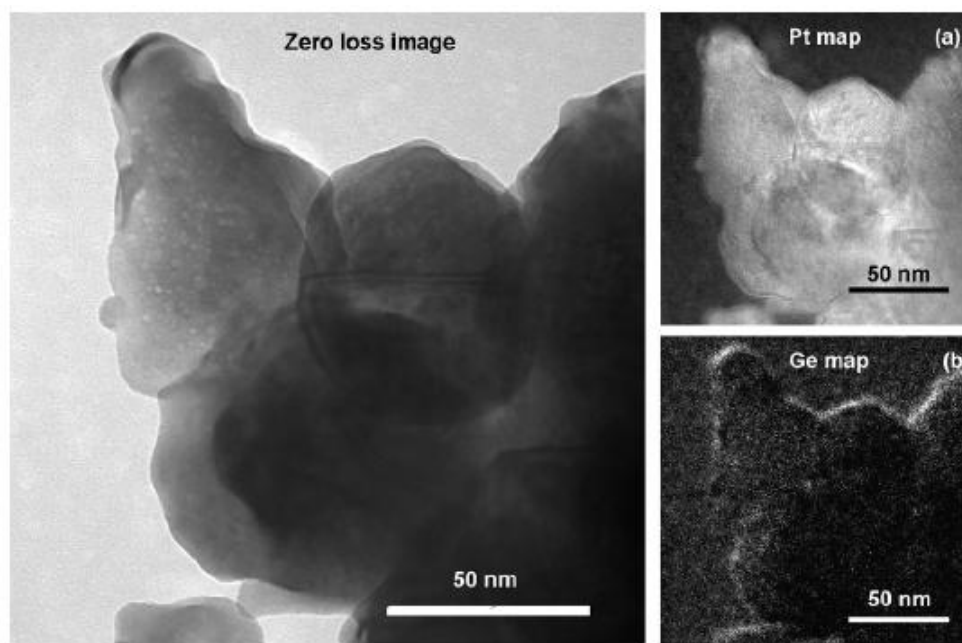

Fig. 3: HRTEM image of **GePt** black catalyst. (a) Pt map and (b) Ge map of the same area (bright streaks) taken from EELS measurement.

saturated products decreased, while the selectivities of hydrogenolysis and unsaturated products increased over **GePt** catalyst. Similar selectivity changes could be observed as a function of hydrogen pressure. The formation of saturated products (MCP and isomers) was suppressed and the overall yield of unsaturated products increased under lower values of hydrogen pressure (Fig. 5).
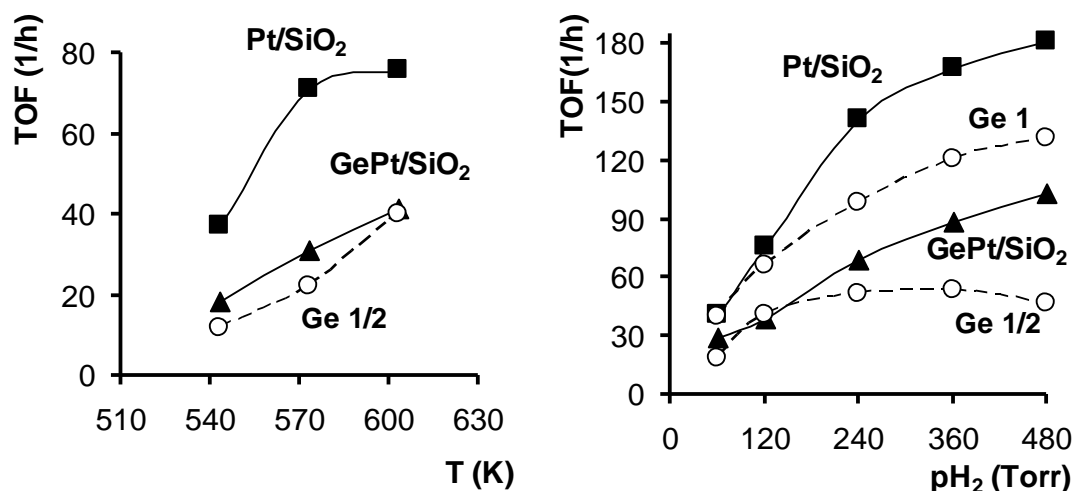
Fig. 4: Turnover frequencies for the conversion of hexane on ■ - **Pt/SiO₂** and ▲ - **GePt/SiO₂** as a function of (a) temperature at p(MCP):p(H₂)=10:120 Torr, t=5 min, (b) hydrogen pressure at T=603 K. ○ − Ge ½ and Ge 1 data taken from Ref [13].
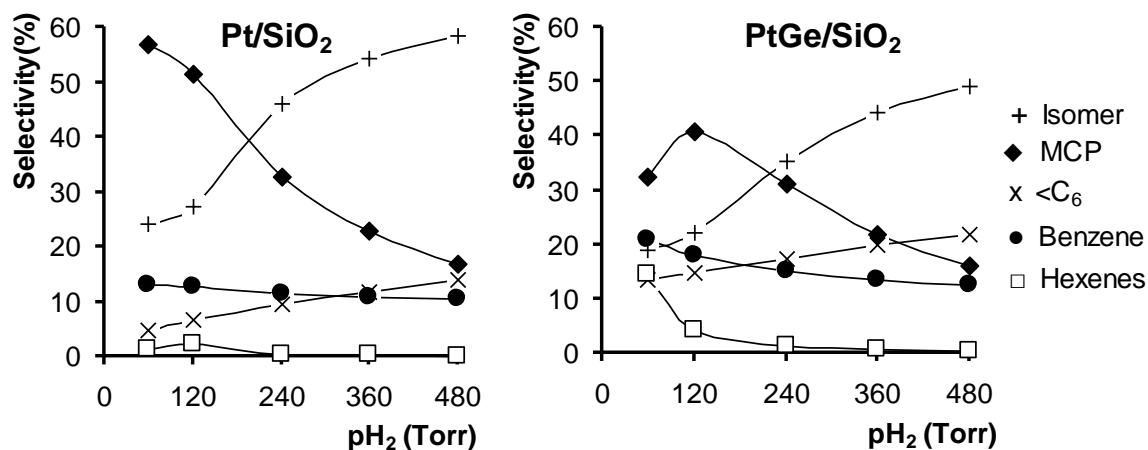
Fig. 5: Comparison of selectivity pattern of hexane reactions on **Pt/SiO₂** and **GePt/SiO₂** at T= 603 K as a function of hydrogen pressure.
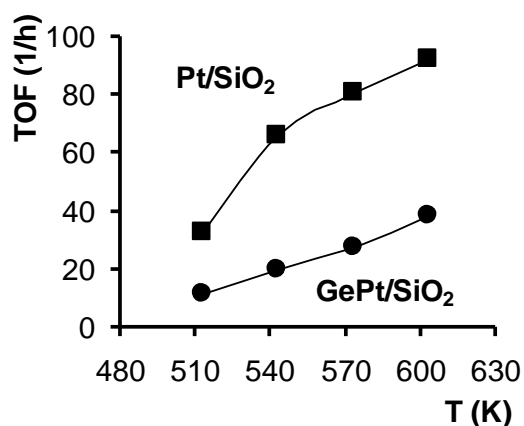
Fig. 6: Conversion of MCP on ■ - **Pt/SiO₂** and ● - **GePt/SiO₂** as a function of temperature (p(MCP):p(H₂)=10:120 Torr, t=5 min)

3.1.4.2 Catalytic reactions of methylcyclopentane on GePt/SiO₂

Ring opening and hydrogenolysis products ($<C_6$) were formed from MCP on both catalysts and also unsaturated products were observed. Ring opening took place in three positions producing 2-methylpentane (2MP), 3-methylpentane (3MP) and hexane (nH), in proportions different from random ring opening [38]. In addition, Pt/SiO₂ and Ge modified Pt/SiO₂ produced also benzene and unsaturated products (mainly hexenes). Figure 6 illustrates how the turnover frequencies for MCP conversion changed on both catalysts as a function of temperature. The activity increased with the reaction temperature, but the turnover frequencies on the bimetallic **GePt** samples were lower in this reaction, too. Figure 7 shows selectivity values as a function of the temperature. In this reaction lower
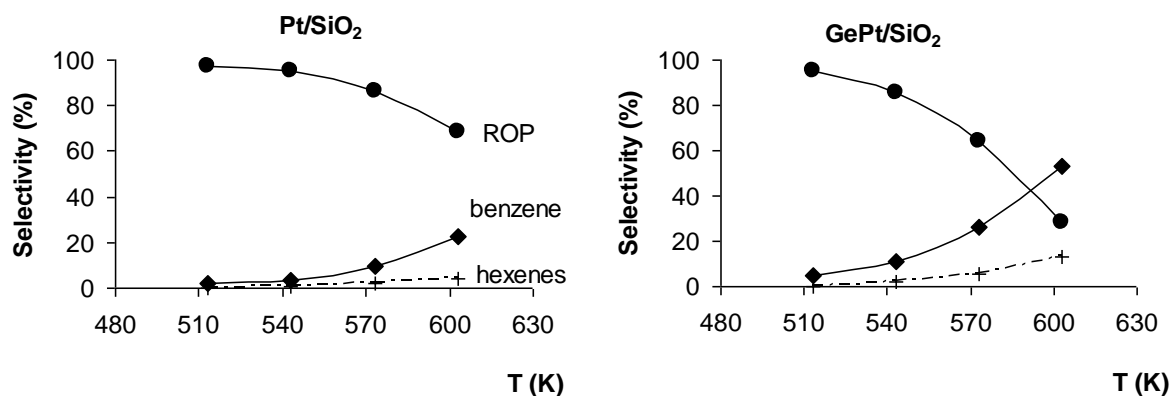
Fig. 7: Selectivity pattern of MCP conversion over **Pt/SiO₂** and **GePt/SiO₂** as a function of temperature at p(MCP):p(H₂)=10:120 Torr.

Table 2: Product selectivities of hexane reactions over SiO₂ supported **Pt** and **GePt** catalysts as a function of temperature [p(nH):p(H₂)=10:120 Torr]

| | Selectivity (%) | | | | | |
| | Pt | | | GePt | | |
Temperature (K)	543	573	603	543	573	603
<C₆	7.1	9.8	7.2	20.8	16.4	16.4
Isomers	36.6	25.3	25.7	35.2	27.1	20.3
Hexenes	–	0.8	1.9	–	1.5	4.1
MCP	49.7	55.6	53.2	35.3	43.4	43.4
Benzene	6.6	8.5	12	8.7	11.6	15.8

Table 3: Ratio of ring opening products of MCP on supported catalysts as a function of temperature (at p(MCP):p(H₂)=10:120 Torr) and hydrogen pressure. Selected typical values are shown.

| | Pt/SiO₂ | | | GePt/SiO₂ | | |
| | 2MP/3MP | 2MP/nH | 3MP/nH | 2MP/3MP | 2MP/nH | 3MP/nH |
Statistical RO	2	1	0.5	2	1	0.5
Temperature (K)						
513	2.7	2.0	0.7	2.8	5.0	1.8
543	2.6	1.7	0.7	2.4	3.0	1.3
573	2.2	1.4	0.6	2.0	2.4	1.1
603	1.9	1.3	0.7	1.7	1.5	0.9
H₂ pressure (Torr) T = 603 K						
60	1.7	1.3	0.7	1.7	1.2	0.7
120	1.9	1.3	0.7	1.7	1.5	0.9
240	2.2	1.3	0.6	1.9	2.3	1.2
360	2.3	1.3	0.6	2.1	2.7	1.3
480	2.3	1.3	0.6	2.3	3.0	1.3
H₂ pressure (Torr) T = 573 K						
60	1.9	1.3	0.7	1.8	1.6	0.9
120	2.2	1.4	0.6	2.0	2.4	1.1
240	2.6	1.4	0.6	2.3	3.8	1.7
360	2.7	1.4	0.5	2.6	4.7	1.8
480	2.8	1.3	0.5	2.8	5.0	1.8

amounts of hydrogenolysis products were formed. The selectivity of <C₆ changed between 0.5-4.5 %, increasing with the temperature. Ring opening was the main reaction on both catalysts. Over **GePt** catalyst the selectivity of saturated products decreased, while the selectivities of benzene and hexenes increased with increasing temperature like in hexane reactions. At 603 K the selectivity of hexenes was three times higher on **GePt** than over **Pt** (Fig. 7). As for the position of ring opening, Gault and co-workers have postulated a "selective" and "nonselective" pathway of the C₅ ring opening [39]. The latter would produce a

statistical distribution of 2MP, 3MP and nH, while much less (or even zero) nH would be produced in the "selective" ring opening. Table 3 shows the selectivity of ring opening products in MCP transformation on **Pt** and **GePt.** The parent **Pt** catalyst was less selective in ring opening reactions and the selectivity was hardly affected by the temperature. The deviation from random ring opening was somewhat larger at 573 K than at 603 K and at higher H₂ pressures. Over bimetallic catalyst the ring opening was rather "selective" at 513 K, while this selective character decreased with increasing temperature and the ring opening became roughly statistical at 603 K, indicating that "adlineation sites" [40] might have been present and active on the Pt/SiO₂ borderline. The selectivities on catalysts were compared as a function of hydrogen pressure at 573 and 603 K. Ring opening selectivities were hardly affected by hydrogen pressure over parent **Pt** catalyst (all ratios were close to statistical), while on **GePt** the ring opening became remarkably selective with increasing p(H₂). The ratio 2MP/3MP was very stable while the MP/nH ratios (chracteristic of the "selective" ring opening showed somewhat larger scattering)

3.1.4.3. GePt black in the catalytic reaction of hexane

Figure 8 shows how the turnover frequencies for hexane conversion changed on both unsupported catalysts as a function of temperature and hydrogen pressure. The turnover frequencies on the bimetallic **GePt** samples were much higher, meaning that the presence of Ge increased the catalytic activity. This is in agreement with the purity of **GePt** (Table 1**;** the O component must have been removed by H₂ in the reaction mixture. Isomerization and C₅-cyclization were the main reactions on both catalysts (Table 4), except on Pt at 603 K, where hydrogenolysis had highest selectivity. The selectivity of saturated products increased, while those of hydrogenolysis and unsaturated products decreased over **GePt** catalyst. Similar tendencies of selectivity changes could be observed as a function of hydrogen pressure. The formation of saturated products
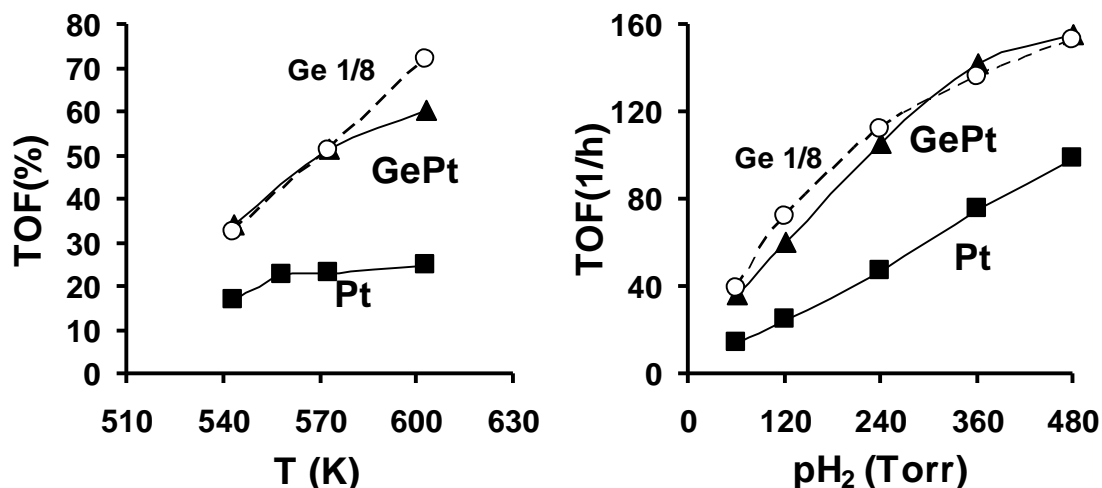
Fig. 8: Turnover frequencies for the conversion of hexane on ■ - **Pt** and ▲ – **GePt** black as a function of (a) temperature at p(MCP):p(H$_2$)=10:120 Torr, t=5 min, (b) hydrogen pressure at T=603 K. ○ − Ge 1/8 data taken from Ref [13].
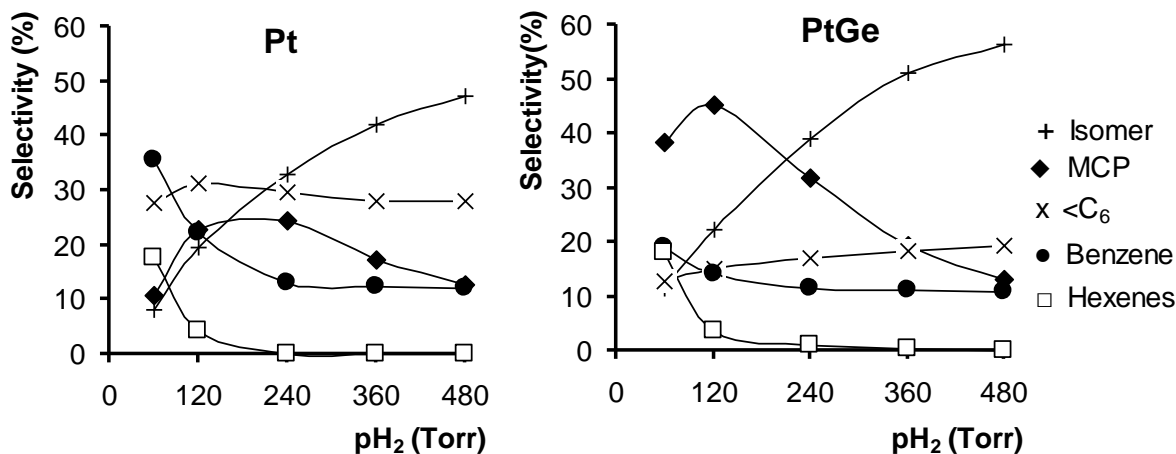
Fig. 9: Selectivity pattern of hexane reactions on **Pt** and **GePt** black at T= 603 K as a function of hydrogen pressure.

(MCP and isomers) increased and the overall yield of unsaturated products decreased (Fig. 9).

4. Discussion

Our previous study [13] revealed that small amounts of Ge (**Ge 1/12** and **Ge1/8**) increased the catalytic activity of Pt and also the selectivities to saturated products (skeletal isomers and MCP) from hexane. The reason was the selective deposition of small amounts of germanium to platinum into positions where reactions requiring multiple sites (fragmentation [41] and aromatization [14]) would occur. In the **Ge1/2** sample, much higher fraction of the surface was covered with inactive Ge, rendering this sample the least active of the series. Samples **Ge1** and **Ge2** contained a high fraction of Ge in deeper layers, forming "bulk bimetallic" catalysts which again contained more

active surface Pt sites [13], but not necessarily with the same selectivities.

Just one bimetallic **GePt** sample was prepared using the method in the present study; the Ge:Pt ratio was constant. The overall activity of **GePt/SiO$_2$** was lower than that of its parent catalyst (Figure 3). The temperature dependence of the activity of our bimetallic sample was closer to that of **Ge1/2** (on Al$_2$O$_3$ support), indicating that the electrochemical deposition introduced sufficient germanium to transform the small Pt particles (3±0.7 nm [16]) to a bimetallic system with random Ge deposition along the whole Pt surface. The hydrogen pressure dependence, in turn, was between the results observed with **Ge1** and **Ge1/2**, i.e., our **GePt/SiO$_2$** was better than **Ge1/2** with randomly deposited Ge on the surface but inferior to **Ge1** where bulk Ge-Pt formation started, liberating some surface Pt sites for catalysis. These sites could be successfully activated by more surface hydrogen. The relatively high frag

Table 4: Product selectivities of hexane reactions over unsupported **Pt** and **GePt** catalysts as a function of temperature [p(nH):p(H$_2$)=10:120 Torr]

	Selectivity (%)					
	Pt			GePt		
Temperature (K)	543	573	603	543	573	603
<C$_6$	20.8	25.4	31.2	14.3	12.6	15.1
Isomers	40.3	31.9	19.7	44.8	30.2	22.1
Hexenes	–	0.4	4.2	–	1.3	3.6
MCP	26.7	29.3	22.8	28.7	44.9	45.1
Benzene	12.2	13	22.1	12.2	11	14.1

mentation selectivity of **GePt/SiO$_2$** (Table 2) and benzene selectivity values were also analogous to earlier results obtained with **Ge1/2** [13]. The saturated products formed over **GePt/SiO$_2$** consisted mainly of MCP (Figure 5) indicating the poorer utilization of higher H$_2$ pressures to create Pt–H sites necessary to promote opening of the MCP ring to isomers. The same conclusions could be drawn from using MCP probe molecules (Figure 7). The selectivity to ring opening products decreased more strongly at higher temperatures with **GePt/SiO$_2$** than with **Pt/SiO$_2$**. The bimetallic catalyst produced more benzene than **Pt/SiO$_2$** whereas the amount of fragments was negligible. This also indicates the presence of smaller, hydrogen-poor active ensembles. Ring opening was not very selective on **Pt/SiO$_2$** (Table 3); lower temperatures and higher hydrogen pressures favouring "selective" ring opening. This situation changed dramatically on **GePt/SiO$_2$**, indicating that adding Ge almost eliminated the role of adlineation sites [40] on the Pt–silica borderline. Another reason for the excess of methylpentanes may be due to the consumption of a fraction of hexane precursors to produce benzene. The fact that no "Pt–Ge borderline effect" arose indicates again the high dispersion of Ge. Since the support was inactive, "Ge-support" interactions did not influence the catalytic properties.

Ge deposition on to the unsupported **Pt** produced a cyclic voltammogram suggesting ca. 40 % surface Ge that would agree well with the Ge content of **Ge1/2**. Our **GePt** black catalyst was, however, better than the parent **Pt** (Figure 9). Its behaviour (Figure 8) was analogous to the second best bimetallic alumina-supported sample, i.e., **Ge1/8** [13]. The selectivities on **GePt** were close to the values measured on **GePt/SiO$_2$**, both as a function of reaction temperature (Tables 2 and 4) and H$_2$ pressure (Figures 5 and 9). These values show a marked improvement of **GePt** as compared to the parent **Pt** black. Deposition of Ge must have prevented accumulation of adventitious C in both cases. This may be a new important statement about these bimetallic catalysts containing low amount of additive.

The electrochemical method, in principle cannot deposit more than 1 monolayer on the parent metal. The catalytic results indicate that the resulting amount of germanium was between ½ and 1 monolayers on SiO$_2$ supported catalyst. This Pt/Ge ratio was far from the optimum on alumina supported catalysts and the results with **GePt/SiO$_2$** were in agreement with this experience. Pt black with small specific surface, in turn, improved markedly upon deposition of Ge, covering, obviously continuous Pt sites favoring deactivation and leaving smaller Pt ensembles active in the desired isomerization–C$_5$-cyclization reactions. Thus, catalytic data indicate low actual surface concentration of Ge. XPS (Table 1) would suggest a Ge/Pt ratio even lower than **Ge1/12**, the majority of Ge being present as Ge^0 (Figure 2a). One has to consider that some platinum must be covered by carbon and some of oxygen is also present on Pt, i.e., the comparison with **Ge1/8** [13] seems to be realistic. These catalytic results are in agreement with the EFTEM pictures (Figure 3), showing contiguous Pt and scattered Ge signal. One must not forget that atomically dispersed Ge would not be able to produce visible signals above detection limit, i.e., the light spots on the Ge map must correspond to small islands representing only a fraction of the total germanium amount. Even the presence of small amount of Ge prevented the appearance of Pt–O$_{ads}$ observed earlier with Pt black exposed to air [19].

Acknowledgement

References

[1] G.A. Mills, H. Heinemann, T. H. Milliken, A. G. Oblad, Ind. Eng. Chem., 45 (1953) 134.

[2] G. J. Antos, A. M. Aitani (Eds.) Catalytic Naphtha Reforming 2nd Ed., Marcel Dekker, 2004.

[3] B. H. Davis, Catal. Today, 53 (1999) 443.

[4] Z. Paál in G. J. Antos, A. M. Aitani (Eds.) Catalytic Naphtha Reforming second ed., Marcel Dekker, 2004, p. 35.

[5] J. H. Sinfelt, in G. Ertl, H. Knözinger, J. Weitkamp (eds.) Handbook of Heterogeneous Catalysis, Vol. 4, Verlag Chemie, Weinheim, 1997, p. 1939.

[6] V. Ponec, G. C. Bond, Catalysis by Metals and Alloys, Stud. Surf. Sci., Catal. Elsevier, Amsterdam, 1995.

[7] R. Mariscal, J. L. Garcia Fierro, J. C. Jori, J. M. Parera, J. M. Grau, Appl. Catal. A General, 327 (2007) 123.

[8] J. Goldwasser, B. Arenas, C. Bolivar, et al. J. Catal. 100 (1986) 75.

[9] A Borgna, T. F. Garetto, C. R. Apesteguia, B. Moraweck, Appl. Catal. A, 182 (1999) 189.

[10] Z. Huang,, J. R. Fryer, C. Park, D. Stirling, G. Webb, J. Catal., 175 (1998) 226.

[11] J. Margitfalvi, M. Hegedüs, S. Göbölös, E. Kern-Tálas, P. Szedlacsek, S. Szabó, F. Nagy, Proc. 8th International Congress on Catalysis, Berlin, 1984, Verlag Chemie,Weinheim, Vol. 4, p. 903.

[12] S. Szabó, Int. Rev. Phys. Chem., 10 (1991) 207.

[13] A. Wootsch, Z. Paál, N. Győrffy, S. Ello, I. Boghian, J. Leverd, L. Pirault-Roy, J. Catal., 238 (2006) 67.

[14] P. Biloen, J. N. Helle, H. Verbeek, F. M. Dautzenberg, W. M. H. Sachtler, J. Catal., 63 (1980) 112.

[15] Z. Paál, N. N. Győrffy, A. Wootsch, L. Tóth, I. Bakos, S. Szabó, U. Wild, R. Schlögl, J. Catal., 250 (2007) 254.

[16] N. Győrffy, A. Wootsch, S. Szabó, I. Bakos, L. Tóth, Z. Paál, Topics Catal., 46 (2007) 57.

[17] Z. Paál, J. Catal. 105 (1987) 540.

[18] G. C. Bond, Metal-Catalyzed Reactions of Hydrocarbons, Springer, New York, 2005.

[19] Z. Paál, U. Wild, A. Wootsch, J. Find, R. Schlögl, Phys. Chem. Chem. Phys. 3 (2001) 2148.

[20] Z. Paál, H. Zimmer, J. R. Günter, R. Schlögl, M. Muhler, J. Catal. 119 (1989) 146.

[21] L. S. Carvalho, C. L. Pieck, M. C. Rangel, N. S. Figoli, J. M. Grau, P. Reyes, J. M.Parera, Appl Catal 269 (2004) 91.

[22] V. A. Drozdov, B. B. Fenelonov, L. G. Okkel, T. I. Gulyaeva, N. V.Antonicheva, N. S. Sludkina, Appl. Catal. A 172 (1998) 7.

[23] J. L. Margitfalvi, I. Borbáth, E. Tfirst, A. Tompos, Catal. Today, 43 (1998) 29.

[24] J. L. Margitfalvi, I. Borbáth, M. Hegedüs, A. Tompos, Appl. Catal. A, 229 (2002) 35.

[25] A. Wootsch, Z. Paál, S. Szabó, I. Bakos, H. Sauer¸ U. Wild¸ R. Schlögl, Appl. Catal. A, 309 (2006) 1.

[26] Z. Paál, R. Schlögl, Surf. Interf. Anal., 19 (1992) 524.

[27] Z. Paál, R. Schlögl, G. Ertl, J. Chem. Soc. Faraday Trans., 88 (1992) 1179.

[28] U. Wild, D Teschner, R. Schlögl, Z. Paál, Catal. Lett., 67 (2000) 93.

[29] Practical Surface Analysis ed. D. Briggs, M. P. Seah Wiley, Chichester, 1990, Appendix 6, Vol. 1, p. 635.

[30] D. Teschner, D. Duprez, Z. Paál, J. Mol. Catal. A 19 (2002) 201.

[31] A. Wootsch, Z. Paál, J. Catal. 205 (2002) 86.

[32] N. Furuya, S. Motoo, J. Electroanal. Chem., 99 (1979) 19.

[33] R. Gomez, M.J. Llorca, J.M. Feliu, A. Aldaz, J. Electroanal. Chem., 340 (1992) 349.

[34] P. Rodriguez, E. Herrero, J. Solla-Gullo, F.J. Vidal-Iglesias, A. Aldaz, J.M. Feliu, Electrochimica Acta, 50 (2005) 3111.

[35] I. Bakos, S. Szabó, F. Nagy, J. Electroanal. Chem., 309 (1991) 293.

[36] N. M. Rodriguez, P. E. Anderson, A. Wootsch, U. Wild, R. Schlögl, Z. Paál, J. Catal.,197 (2001) 365.

[37] M. Muhler, Z. Paál, R. Schlögl, Appl. Surface Sci., 47 (1991) 281.

[38] F. G. Gault, Adv. Catal. 30 (1981) 1.

[39] G. Maire, G. Plouidy, J. C. Prudhomme, F. G. Gault, J. Catal. 4 (1965) 556.

[40] H. Glassl, K. Hayek, R. Kramer, J. Catal. 68 (1981) 397.

[41] J. H. Sinfelt, Adv. Catal. 23 (1973) 91.